10

IP switch and big bend

Contents

10.1 Introduction

The IP switch follows the main linac and collimation section and allows slow switching between multiple IPs. The big bend provides muon protection and IP separation. It also generates the IP crossing angle which facilitates extraction of the spent beams. Figure 10-1 shows a schematic layout (drawn to scale) of the IP switch, the two big bend sections, and the skew correction and diagnostic sections (Chapter 11). These sections follow the collimation section (Chapter 9) and a 100-m-long emittance diagnostic section. An NLC design with two IPs will require two IP switches and four big bends.

10.2 The IP Switch

The purpose of the IP switch is to provide capability for switching the beam between two alternate final focus beam lines. The IP switch should provide enough separation so that most of the major transport elements are not shared by the two beam lines. Rapid switching of the beam between alternate transport lines is not necessary. It is probably possible to make the switch in a period of less than one hour. Emittance growth from aberrations and synchrotron excitation should be negligible (*i.e.,* a few percent).

10.2.1 Optics Design

The IP switch bends the beam a total of 1.5 mr. Figure 10-2 shows the IP switch optics. The QS quadrupole is horizontally movable in order to switch between IPs. It is displaced by ± 3.25 cm (± 2.6 cm) for the 500-GeV/beam (750-GeV/beam) configuration.

The upgrade to 750 GeV/beam is accomplished by adding ten 3-m-long dipoles inboard of the existing dipoles (Figure 10-3a and 10-3b). Some quadrupole strength changes are also necessary. Figure 10-3 shows the beam line offsets for the 500-GeV/beam (Figure 10-3a) and the 750-GeV/beam (Figure 10-3b) cases. The plots start from the end of the collimation section and continue through the big bend matching section. The BS dipoles should be thin C-magnet types to fit in the 11.7-cm (7.8-cm) center-to-center separation at the face of the first dipole just downstream of the QS quadrupole. The first five BS dipoles (first ten for the 750 GeV/beam configuration) provide the separation, while the QS quadrupole and the next five (ten) BS dipoles make the system achromatic. Beam line elements through QS are common to both beam lines. Three configuration modes are possible. The first is at 500 GeV/beam with 10 dipole magnets installed (Figure 10-3a), the second is at 500 GeV/beam with 20 dipole magnets installed (Figure 10-3b), and the third is 750 GeV/beam with 20 dipole magnets installed (also Figure 10-3b). Tables 10-1 and 10-2 list the magnets for both energies. The match into the IP switch and also into the big bend has been accomplished with two sets of four quadrupoles (QM1,…8) of modest design. The center-to-center separation at the face of QM5 is 15.7 cm, requiring a special thin quadrupole design at least for QM5 and QM6.

10.2.2 Chromatic Emittance Dilution

Tracking studies using the tracking code TURTLE [Carey 1982] have been made for beams with Gaussian energy distributions having rms of 0.2, 0.4, and 0.6%. The results for the entire beam line (from end of collimation section

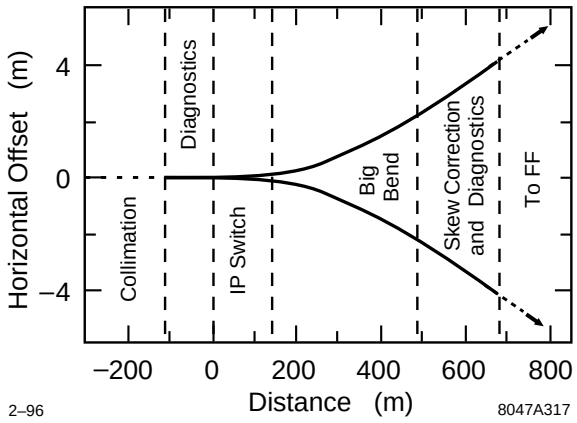

Figure 10-1. *IP switch/big bend layout (to scale).*

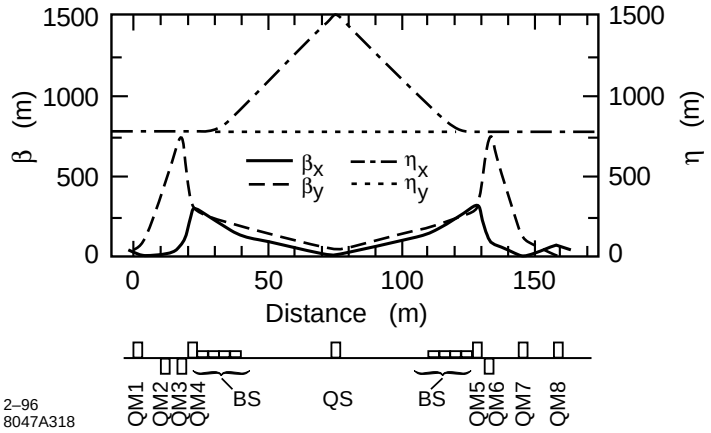

Figure 10-2. *IP Switch Optics (500 GeV/beam).*

Name	Number	Length (m)	Radius (mm)	Pole-Tip Field (kg)
QM1	1	2.5	6	+5.85 (+8.78)
QM2	1	2.5	6	−0.33 (−0.38)
QM3	1	2.5	6	−6.57 (−10.0)
QM4	1	2.5	6	+6.62 (+9.97)
QS	1	2.0	6	+2.35 (+4.43)
QM5	1	2.5	6	+6.08 (+9.15)
QM6	1	2.5	6	−6.60 (−9.97)
QM7	1	2.5	6	+3.01 (+4.62)
QM8	1	2.5	6	+6.66 (+10.0)

Table 10-1. *IP-switch quadrupole magnets for 500 GeV/beam (750 GeV/beam). Fields for the 20-dipole, 500-GeV/beam mode (not shown) are simply scaled from the 750-GeVcase.*

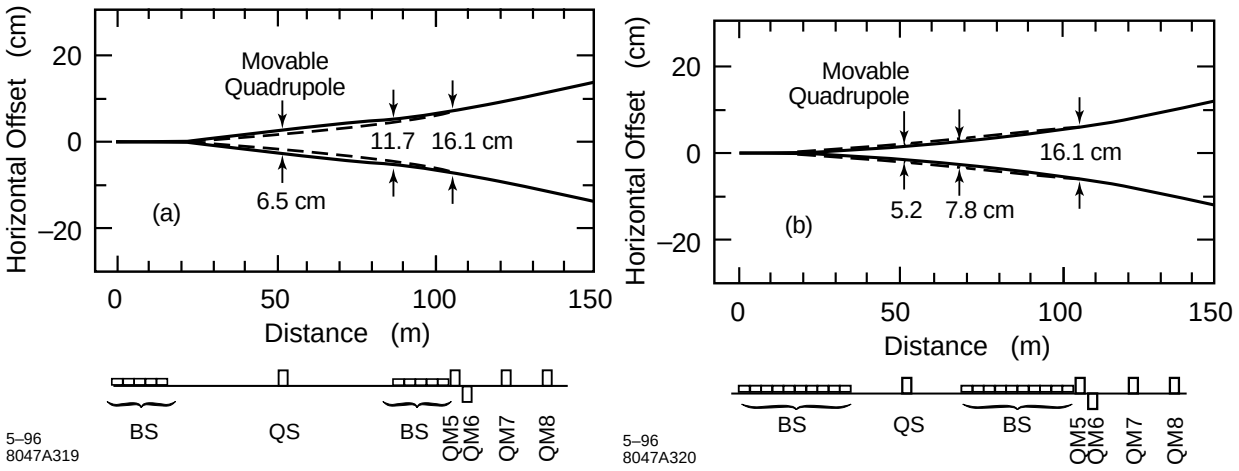

Figure 10-3. *(a) IP switch beam line (500 GeV/beam). Dashed line is nominal beam line at 750 GeV. (b) IP switch beam line at 750 GeV/beam after adding 10 more 3-m dipoles inboard of existing dipoles. Dashed line is nominal beam line at 500 GeV/beam.*

Beam Energy (GeV)	Name	Number	Length (m)	Half Gap (mm)	Field (kGauss)
500	BS	10	3.0	6	0.834
500	BS	20	3.0	6	0.417
750	BS	20	3.0	6	0.625

Table 10-2. *IP switch dipole magnets for different energy modes.*

to beginning of final focus) are tabulated in Table 10-9. The chromatic contribution to emittance increase for the IP switch alone at 0.3% rms energy spread is <1% in each plane.

10.2.3 Synchrotron Radiation

The horizontal emittance dilution, energy spread increase, and energy loss due to synchrotron radiation (SR) through the IP switch are summarized in Table 10-3. The 7.3% emittance increase quoted in Table 10-3 is with respect to the main damping ring extracted emittance. For a more realistic end-of-linac emittance of $\gamma\epsilon_{x0} = 5 \times 10^{-6}$ m the increase is 4.4%.

10.2.4 Tolerances

The single-element tolerances for the IP switch magnets are listed in Tables 10-4 (dipoles) and 10-5 (quadrupoles). Each tolerance represents a 2% luminosity loss for that single element's effect on one beam. The effects of these errors generally increase the IP beam size except in the case of dipole field regulation and quadrupole transverse vibration which continuously steer the beams out of collision. In this case, since the exact betatron phase to the IP is

Beam Energy (GeV)	Number of Dipoles	$\Delta\epsilon_{x\mathrm{SR}}/\epsilon_{x0}$ (%)	$\sigma_{\delta\mathrm{SR}}$ (10^{-4})	Energy loss (MeV)
500	10	3.3	7	66
500	20	0.7	3	33
750	20	7.3	10	167

Table 10-3. *Horizontal emittance dilution, energy spread increase and energy loss due to synchrotron radiation through the IP switch ($\gamma\epsilon_{x0} = 3 \times 10^{-6}$ m).*

NAME	Quantity	roll (mr)	$\Delta B/B_0$ (%)	b_1/b_0 (%)	b_2/b_0 (%)
BS	10	10	0.033	3.4	300

Table 10-4. *IP switch dipole magnet single element tolerances at 500 GeV/beam for 2% luminosity loss each ($\gamma\epsilon_{x0} = 3 \times 10^{-6}$ m, $\gamma\epsilon_{y0} = 3 \times 10^{-8}$ m, $\sigma_\delta = 0.3\%$). Quadrupole and sextupole field harmonics (b_1/b_0 and b_2/b_0) are evaluated at a radius of 4 mm. The sextupole field harmonics for the dipoles are extremely loose ($\sim 300\%$ at $r = 4$ mm).*

NAME	Quantity	roll (mr)	Δx offset (μm)	Δy offset (μm)	Δx_{rms} vibrate (μm)	Δy_{rms} vibrate (μm)	$\Delta B/B_0$ (%)	b_2/b_1 (%)
QM1	1	4.1	360	21	1.1	0.063	4.5	1650
QM2	1	27	6800	130	20	0.400	11	4000
QM3	1	0.47	150	5.2	0.45	0.016	0.33	55
QM4	1	0.40	83	7.9	0.25	0.024	0.56	52
QS	1	1.2	1680	76	5.0	0.230	5.1	150
QM5	1	0.43	90	8.7	0.27	0.026	0.61	58
QM6	1	0.46	150	5.2	0.44	0.016	0.33	55
QM7	1	12	1500	30	4.5	0.090	4.9	3750
QM8	1	7.2	190	61	0.58	0.180	4.5	1000

Table 10-5. *IP switch quadrupole magnet single element tolerances at 500 GeV/beam for 2% luminosity loss each ($\gamma\epsilon_{x0} = 3 \times 10^{-6}$ m, $\gamma\epsilon_{y0} = 3 \times 10^{-8}$ m, $\sigma_\delta = 0.3\%$). Sextupole field harmonics (b_2/b_1) are evaluated at a radius of 4 mm and are very loose ($> 50\%$).*

not calculated, phase averaging is applied. The tolerances given in the tables have not yet been distributed out into a weighted tolerance budget; the numbers are for reference. In fact, given multiple errors over multiple elements, these tolerances are much too loose. However, since tuning considerations have not been folded in, most static, non-steering errors may also be corrected over some reasonable range.

10.2.5 Diagnostics and Correctors

Beam position monitors (BPM) will be required, probably one horizontal and one vertical BPM per $\pi/2$ of betatron phase. A minimal number of dipole orbit correctors should be used; the optimal locations for these devices have yet

to be established. The diagnostic section at the end of the big bend will be used to determine the quality of the match into the big bend.

The horizontal dispersion of 32 mm (26 mm at 750 GeV/beam) at QS provides an excellent location for the measurement of beam energy and energy spread, using a BPM and a profile measurement device such as a wire scanner. At the entrance to QS, the dispersive horizontal spot size for a beam with 0.3% rms energy spread is 96 μm (78 μm), while the betatron spot size ($\gamma\epsilon_x = 3 \times 10^{-6}$ m) at this location is only 5.2 μm (4.2 μm), allowing a good energy spread measurement. In addition, placement of a 1-μm-resolution BPM at this location will provide a relative energy measurement resolution of $\sim 3 \times 10^{-5}$.

10.2.6 Beam Correction Issues

Beam-based techniques will be used to verify transverse alignment during commissioning of the beam line, but will probably be infrequently necessary thereafter. Orbit correction algorithms remain to be studied, but a simple point-to-point scheme will probably be sufficient. Feedback stabilization of beam position at the entrance to the big bend will probably be desirable, depending on the stability of the incoming beam.

10.2.7 Other Issues

Some issues remain to be considered, including:

- The need for machine protection collimators and their locations.
- Vacuum and pumping requirements.

10.3 The Big Bend

The big bend is a low-angle arc after the main linac which provides detector muon protection [Keller 1993], an IP crossing angle to facilitate extraction of the spent beams, and allows switching between multiple IPs. The total bend angle (including 1.5-mr IP switch angle) is 10 mr (20-mr IP crossing angle) which provides ∼40-m spatial separation between the two IPs (∼700-m transport to an ∼1600-m-long final focus). At 500–750 GeV/beam, the horizontal emittance growth due to SR sets lower limits on the system design length. The following Section describes an optimized optical design of this big bend section for 500 GeV/beam and 750-GeV/beam electrons (or positrons).

10.3.1 Optical Design

For electrons, the emittance growth due to SR is calculated using [Helm 1973, Raubenheimer 1993]:

$$\Delta\gamma\epsilon_x \approx \left(4 \times 10^{-8}\,\mathrm{m^2\,GeV^{-6}}\right) \cdot E^6 \sum_i \frac{L_i \langle H \rangle_i}{|\rho_i|^3} \quad , \tag{10.1}$$

where the summation is over bending magnets, L is the magnet length, ρ is the bend radius of the magnet, E is the beam energy, and $< H >$ is the mean of the usual "curly-H" function.

$$\langle H \rangle = \frac{1}{L} \int_0^L \frac{\eta^2 + (\eta\prime\beta + \eta\alpha)^2}{\beta} dz \tag{10.2}$$

This integral has been solved [Helm 1973] for a magnet with bending and focusing. The mathematical result is lengthy and is not reproduced here. To find the optimal parameters for a string of FODO cells, this result is used with Equation (10.1) in a convenient computer program to calculate the SR emittance growth with maximum quadrupole pole-tip fields of 10 kg at 750 GeV/beam with a 6-mm radius. Preliminary resistive wall calculations [Bane 1995] indicate that this radius might be decreased to 3 mm, shortening the system length by ∼100 m. However, it is thought that this possibility may not provide an adequate safety factor.

The number of FODO cells and the phase advance per cell are varied to find the minimum total length for a ∼2% horizontal SR emittance growth ($\gamma\epsilon_{x0} = 3 \times 10^{-6}$ m). Both separated function and combined function magnet systems were explored. The parameters reached represent a compromise between theoretical optimal values and realistic constraints on magnet lengths and reasonable phase advance per cell.

The phase advances per cell chosen ($\Psi_x = 108°, \Psi_y = 90°$) do not represent the precise optimum ($\Psi_x = 135°, \Psi_y < 72°$). The values are biased towards a more reasonable design considering beam position monitor sampling, chromaticity, a potential sextupole resonance and magnet alignment tolerances. The effect on the total length of this slight bias is small (<10%). Splitting the horizontal and vertical tunes in the separated function lattice improves the bending magnet density because it allows the D-quadrupoles to be shorter than the F-quadrupoles for a constant pole-tip field. However, in a combined function design, this split does not improve the SR emittance dilution. The tune split may also desensitize the beam to a potential ion instability. The choice between combined function (CF) or separated function (SF) lattice reduces to a few points listed below.

Combined Function: The CF lattice is more space-efficient and only one type of magnet needs to be built. The main disadvantage is that the focusing strength is not tunable without changing the bending strength. The magnets are long (∼6 m) since they bend and focus, but the net length is still shorter than the SF design (∼30%).

Separated Function: In its favor, the SF lattice may be more easily tuned since the focusing strength will be independent of the bend strength. For example, the phase advance per cell may be changed to provide a trombone tuner between the collimation phase and the IP. Also beam-based alignment techniques can be applied. However, there are three types of magnets to build in this scheme and the overall length needs to be longer than the CF design (∼30%).

Due to its tunability and beam-based alignment potential, we have chosen the SF design. The dispersion and beta functions of the 500-GeV/beam SF design are shown in Figure 10-4. The final design uses 15 FODO cells with four dipoles per cell. Table 10-6 lists the FODO parameters for the big bend SF design.

A 76-cm quadrupole-to-dipole space has been maintained for BPM and ion pump placement and a 50-cm dipole-to-dipole space is held so that the dipole and quadrupole magnet lengths are no more than 3 m and 2.5 m, respectively. A "missing-magnet" dispersion matcher/suppressor is used at the entrance and exit of the FODO string. The matcher/suppressor magnets are identical in size and strength to those in the FODO section. Only their longitudinal position has been adjusted to obtain the periodic dispersion function in the FODO section. In this way, all 64 dipoles may be powered in series with one power supply, the 17 defocusing quadrupoles powered with a second supply, and the 16 focusing quadrupoles on a third. This allows tuning of the phase advance per cell independently in each plane. Table 10-7 lists the dipole magnet parameters and Table 10-8 lists the quadrupole magnet parameters for the big bend as shown in Figure 10-4. The 3-m-long dipole magnet design may also be used in the IP switch as long as it is a C-magnet design with dimensions which meet the requirements described in Section 10.2.1. The 2.5-m-long QF design may be used for the QM1-8 matching quadrupoles in the IP switch. The center-to-center beam line separation between

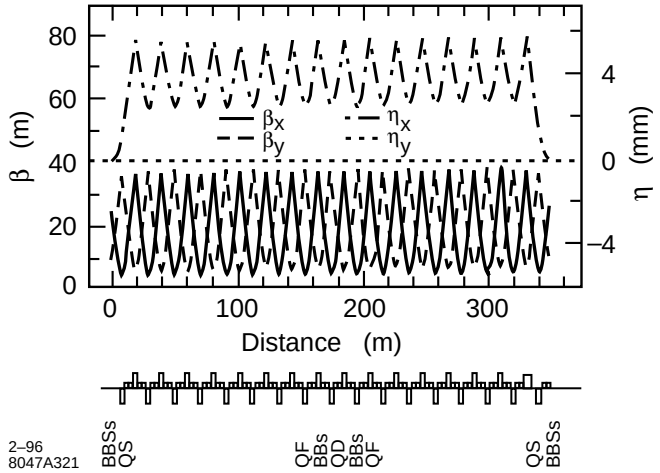

Figure 10-4. *Big bend optics for separated function lattice.*

Total Length (FODO cells)	(m)	312
Total bend angle	(mr)	8.5
Number of FODO cells [a]		15
Maximum $\beta_{x,y}$	(m)	36
Maximum η_x	(mm)	5.6
x-phase advance/cell	(°)	108
y-phase advance/cell	(°)	90
Spin phase advance/cell	(°)	37 (55)
Dipole magnet length	(m)	3.0
Bend radius (per dipole)	(km)	22.6
F-quad length	(m)	2.50
D-quad length	(m)	2.26

[a] There are four dipole magnets per cell.

Table 10-6. *Optimized big bend parameters at 500 GeV/beam (750 GeV/beam) for 6.7-kGauss (10-kGauss) quadrupole pole-tip fields at 6 mm radius and tolerable SR emittance growth.*

the two big bends at the face of the first QD magnet is 28.8 cm (for either 10 or 20 IP switch dipoles) which sets an upper limit on the outer horizontal dimension of the big bend quadrupole magnets of $<$28 cm full width.

10.3.2 Chromatic Emittance Dilution

Tracking studies using TURTLE [Carey 1982] have been made for the entire beam line described in this chapter (nearly 800 meters of beam line from the end of the collimation section to the beginning of the final focus). A Gaussian energy distribution with rms of 0.2%, 0.4%, and 0.6% energy spread was used. For all cases, the emittances used were $\gamma\epsilon_{x0} = 3 \times 10^{-6}$ m and $\gamma\epsilon_{y0} = 3 \times 10^{-8}$ m. The chromatic emittance dilution at 500 GeV/beam for each case is listed in Table 10-9 (SR effects not included). Sextupole compensation is not necessary.

Name	Number	Length (m)	Half Gap (mm)	Field (kGauss)
BB	64	3.0	6	0.738 (1.108)

Table 10-7. *Big bend dipoles for 500 GeV/beam (750 GeV/beam).*

Name	Number	Length (m)	Radius (mm)	Pole Tip Field (kGauss)
QD	17	2.258	6	-6.70 (-10.05)
QF	16	2.500	6	+6.70 (+10.05)

Table 10-8. *Big bend quadrupoles for 500 GeV/beam (750 GeV/beam).*

Rms energy spread (%)	$\Delta\epsilon_x/\epsilon_{x0}$ (%)	$\Delta\epsilon_y/\epsilon_{y0}$ (%)
0.2	1.2	0.2
0.4	3.7	1.6
0.6	7.7	4.2

Table 10-9. *Chromatic emittance increase at 500 GeV/beam for various rms Gaussian energy spreads for beam line including initial diagnostic section, IP switch, all matching sections, big bend, and the skew correction and diagnostic section (synchrotron radiation effects not included).*

10.3.3 Synchrotron Radiation Effects

Optics

Table 10-10 lists the SR parameters for the 500-GeV/beam big-bend design of Figure 10-4. The 750 GeV/beam parameters are also given. The fractional emittance growth referred to is the main damping ring extracted emittance of $\gamma\epsilon_x = 3 \times 10^{-6}$ m. The energy loss across the length of the big bend is 0.07% at 500 GeV (0.22% at 750 GeV). Given the large chromatic bandpass of the big bend (less than 2% emittance increase at 1% rms Gaussian energy spread), it is not necessary to taper the fields through the system.

Beam Energy	(GeV)	500	750
Critical Energy (u_c)	(MeV)	12	42
SR-generated rms Energy Spread	(%)	0.015	0.040
Energy Loss	(GeV)	0.331	1.675
Horizontal SR Emittance Growth	(%)	0.3	3.3
Number of photons/electron		90	456

Table 10-10. *Synchrotron radiation parameters for big bend at 500 GeV and 750 GeV/beam for $\gamma\epsilon_x = 3 \times 10^{-6}$ m.*

NAME	Quantity	roll (mr)	$\Delta B/B_0$ (%)	b_1/b_0 (%)	b_2/b_0 (%)
BB	64	45	0.014	35.0	7500

Table 10-11. *Big bend dipole magnet single-element tolerances at 500 GeV/beam for 2% luminosity loss each ($\gamma\epsilon_{x0} = 3\times10^{-6}$ m, $\gamma\epsilon_{y0} = 3\times10^{-8}$ m, $\sigma_\delta = 0.3\%$). Quadrupole and sextupole field harmonics (b_1/b_0 and b_2/b_0) are evaluated at a radius of 4 mm. The sextupole component tolerances for the dipoles at $r = 4$ mm are extremely loose.*

Detector Backgrounds

The energy distribution generated by SR has a long tail which falls off rapidly for energies, u, well above the critical energy, u_c ($u/u_c \equiv \xi >> 1$) [Sands 1970].

$$n(\xi) \propto \xi^{-1/2} e^{-\xi} \tag{10.3}$$

To estimate the number of electrons in the tail which achieve an oscillation amplitude comparable to one rms horizontal beam size (in the interest of staying clear of the final doublet face), the necessary energy deviation, u_1, is written in terms of the rms SR energy spread, σ_δ, the relative horizontal SR emittance increase, $\Delta\epsilon_x/\epsilon_{x0}$, and the beam energy, E_0.

$$\xi_1 \equiv \frac{u_1}{u_c} = \frac{\sigma_\delta}{u_c/E_0} \cdot \frac{1}{\sqrt{\Delta\epsilon_x/\epsilon_{x0}}} \sim 40 \ (\text{at } E_0 = 750\,\text{GeV}) \tag{10.4}$$

For the worst case (750 GeV/beam), a particle which is 40 critical energies lower than nominal will oscillate at one sigma. The number of electrons per bunch at or beyond this energy, N_{e^-}, is calculated in Equation (10.5) where N_γ is the total number of photons/e^-. Even for 10^{10} electrons per bunch at 750 GeV/beam, this energy tail is insignificant and will not generate a background.

$$N_{e^-} = 10^{10} \cdot \frac{9\sqrt{2}}{15} N_\gamma \int_{\sqrt{2\xi_1}}^{\infty} e^{-x^2/2} dx \sim 10^{-4} \tag{10.5}$$

10.3.4 Tuning, Tolerances, and Corrections

The single-element tolerances for the big bend magnets are listed in Tables 10-11 (dipoles) and 10-12 (quadrupoles). Each tolerance represents a 2% luminosity loss for that single element's effect on one beam. The effects of these errors generally increase the IP beam size except in the case of dipole field regulation and quadrupole transverse vibration which continuously steer the beams out of collision. In this case, since the exact betatron phase to the IP is not calculated, phase averaging is applied. The tolerances given in the tables have not yet been distributed out into a weighted tolerance budget; the numbers are for reference. In fact, given multiple errors over multiple elements, these tolerances are much too loose. However, since tuning considerations have not been folded in, most static, non-steering errors may also be corrected over some reasonable range.

At this time, detailed tolerance and tuning studies have not been performed. However, the big bend design must include dispersion tuning elements for both planes and betatron phases to correct any residual dispersion due to magnet misalignments and gradient errors. Coupling and matching corrections as well as diagnostics exist just after the big bend (Chapter 11). Vertical dispersion correction can be provided by adding four small skew quadrupoles (of zero nominal field)—one per cell in the last four cells. This scheme takes advantage of the 90° vertical phase advance per cell by pairing skew quadrupoles at $-I$ transfer matrix (2 cell) separation so that, for equal and opposite skew quadrupole settings, no betatron cross-plane coupling is generated. The second pair of skew quadrupoles then handles

NAME	Quantity	roll Δx (mr)	Δy offset (μm)	$\Delta x_{\rm rms}$ offset (μm)	$\Delta y_{\rm rms}$ vibrate (μm)	$\Delta B/B_0$ vibrate (μm)	b_2/b_1 (%)	(%)
QD	17	4.4	680	26	2.1	0.077	6.9	2400
QF	16	4.3	230	57	0.70	0.170	3.5	500

Table 10-12. *Big bend quadrupole magnet single-element tolerances at 500 GeV/beam for 2% luminosity loss each ($\gamma\epsilon_{x0} = 3 \times 10^{-6}$ m, $\gamma\epsilon_{y0} = 3 \times 10^{-8}$ m, $\sigma_\delta = 0.3\%$). Sextupole field component tolerances (b_2/b_1) are evaluated at a radius of 4 mm and are very loose ($\geq 500\%$).*

Quad Type	Quantity	Length (m)	pole radius (mm)	max. field (kGauss)	rms reg. tolerance (%)	$\Delta\eta_{x,y}^{\rm max}$ at $\beta_{x,y}^{\rm max}$ (mm)	max. ϵ_y/ϵ_{y0}
skew	4	0.5	6	± 5	0.1	4.6	13
normal	4	0.5	6	± 8	0.5	14	5.1

Table 10-13. *Big bend dispersion tuning magnet specifications at 500 GeV/beam for 0.3% rms energy spread, $\gamma\epsilon_{x0} = 3\times10^{-6}$ m and $\gamma\epsilon_{y0} = 3\times10^{-8}$ m. There is one skew quadrupole in each of the last four FODO cells 10 cm downstream of the QD and one normal quadrupole in each of cells 9, 10, 14 and 15 at 10 cm upstream of the QF.*

the other betatron phase. The range of correction for one pair of 50-cm-long, ± 5-kGauss pole-tip field, 6-mm pole-tip radius skew quadrupoles located 10 cm downstream of each QD at $\beta_y = 32$ m, $\eta_x = 2.8$ mm is $\epsilon_y/\epsilon_{y0} = 13.4$ at 0.3% rms energy spread for $\gamma\epsilon_{y0} = 3 \times 10^{-8}$ m at 500 GeV/beam (the vertical dispersion induced at the center of a QD magnet is as much as 4.6 mm). No significant coupling or horizontal beta function perturbation is generated over this range. However, for very large corrections some second order dispersion may be induced which will limit the correction range or require similar skew sextupole tuners. This level has not yet been studied.

The horizontal dispersion may be controlled similarly by adding two pairs of small normal quadrupoles (of zero nominal field). Due to the 108° horizontal phase advance per cell these quad pairs must be spaced by 5 cells to provide a $-I$ separation. If the 9th and 10th as well as the 14th and 15th cell include a 50-cm-long, ± 8-kg, 6-mm-radius quadrupole which is 10-cm upstream of each QF (at $\beta_x = 31$ m, $\eta_x = 5.2$ mm) the emittance correction range per pair will be $\epsilon_x/\epsilon_{x0} = 5.1$ (the additional horizontal dispersion induced at the center of a QF magnet is as much as 14 mm). However, since the vertical transfer matrix between paired normal quadrupoles (5 cells) is not equal to $-I$, there will be a small perturbation to the vertical beta function which amounts to a 10% beta beat amplitude at full horizontal dispersion correction (± 8 kGauss quadrupole fields). This small effect is correctable with the matching quadrupoles just upstream of the pre-final focus emittance diagnostic section (Chapter 11). The dispersion correction specifications are summarized in Table 10-13.

Given the dispersion correction available, the big bend quadrupoles will probably not require movers. However, beam-based alignment techniques will greatly benefit in speed and convergence if movers (at least in the vertical plane) are available. The movers should control the vertical position to $\sim$5-μm resolution over a range of approximately $\pm 500\,\mu$m. Roll control is not required given the fairly loose roll tolerances as well as the skew (Chapter 11) and vertical dispersion corrections available. Beam-based alignment of the big bend quadrupoles has not yet been studied in detail. However, an independent partial current shunting switch across each big bend quadrupole will probably be a significant advantage for any beam-based alignment algorithm.

Horizontal and vertical dipole correctors at each QF and QD, respectively, will be required to initially steer the beam line and to use in fast feedback applications. Correctors with ± 1.0-kg fields and 25-cm length will be adequate to displace the beam nearly $\pm 500\,\mu$m at the next similar quadrupole at 500 GeV/beam. The horizontal correctors will

then need to regulate at $\sim 1 \times 10^{-3}$ over the 100-ms (10 pulse) range while similar vertical correctors will need $\sim 1 \times 10^{-4}$ regulation ($\sim$0.3% luminosity loss due to all correctors in both big bends for both planes).

The tolerance on the beta match into the big bend is quite loose. It can be shown that the SR emittance increase approximately scales with the amplitude of the incoming beta mismatch.

$$\Delta\varepsilon_{SR} \approx B_{\rm mag}\Delta\epsilon_{\rm SR-nom.} \tag{10.6}$$

Here $B_{\rm mag}(\geq 1)$ is the beta mismatch amplitude in the horizontal plane and $\Delta\varepsilon_{\rm SR-nom.}(\ll \varepsilon_{x0})$ is the nominal SR emittance increase for a matched incoming beam. A very large mismatch of $B_{\rm mag} = 2$ $(\beta_x \approx 4\beta_{x0}, \alpha_x = \alpha_{x0} = 0)$ will amplify a nominal 0.3% SR emittance increase to 0.6%. The vertical match has no such constraint.

10.3.5 Spin Transport and Depolarization

The spin phase advance per cell (spin tune) has also been tabulated in Table 10-6. A spin tune-betatron tune resonance is to be avoided, or small vertical oscillations will precess the electron spin into the vertical plane [Limberg 1993]. However, even without a resonance there may be significant vertical alignment error induced spin rotation due to the large gradient magnets and the extremely high energy. A 100-μm vertical beam offset at 500 GeV/beam in a single QD magnet will rotate a longitudinally oriented spin vector 1° into the vertical plane. If the errors are static this may be compensated by properly orienting the incoming spin vector using the 2-GeV solenoid rotator system (Chapter 5).

The depolarization for a bend through θ, at an energy γ, and an incoming Gaussian rms energy spread of σ_δ is

$$\overline{P}/P_0 = \frac{1}{\sqrt{2\pi}\sigma_\delta}\int_{-\infty}^{\infty} e^{-\delta^2/2{\sigma_\delta}^2}\cos(a\gamma\delta\theta)d\delta = e^{-(a\gamma\theta\sigma_\delta)^2/2} \quad . \tag{10.7}$$

where $a = (g-2)/2$ is the anamolous magnetic moment. For a 10-mr bend at 500 GeV/beam with a 0.3%-rms energy spread the relative depolarization is 0.06% (0.13% at 750 GeV).

10.3.6 Vacuum System

The pressure requirements for the big bend section are set by tolerable detector background levels [Irwin 1993]. At present, it is desirable to achieve an average pressure of $\sim 5 \times 10^{-8}$ Torr in the big bend. If the chamber is cylindrical and made of aluminum with specific outgassing rate $q = 5 \times 10^{-10}$ T-l/s-m (similar to mature SLC arcs), a specific conductance for a 6-mm-radius of $c = 0.18$ m-l/ and ion pumps of speed $S > 5$ l/s placed three per FODO cell ($L \sim$7 m for a total of 45 ion pumps), the system is conductance-limited with average pressure [Ziemann 1992].

$$\overline{P} \cong qL^2/3c \approx 5 \times 10^{-8}\text{Torr} \quad . \tag{10.8}$$

An order-of-magnitude-lower pressure is probably achievable by using a baked stainless steel chamber with a much lower specific outgassing rate.

References

[Keller 1993] L.P. Keller, "Muon Background in a 1.0-TeV Linear Collider", SLAC–PUB–6385 (October 1993).

[Helm 1973] R.H. Helm, M.J. Lee, P.L. Morton, M. Sands, "Evaluation of Synchrotron Radiation Integrals", SLAC–PUB–1193 (March 1973).

[Raubenheimer 1993] T.O. Raubenheimer, P. Emma, S. Kheifets, "Chicane and Wiggler Based Bunch Compressors for Future Linear Colliders", SLAC–PUB–6119 (May 1993).

[Bane 1995] K. Bane, private communication (1995).

[Sands 1970] M. Sands, "The Physics of Electron Storage Rings", SLAC–121 (November 1970).

[Limberg 1993] T. Limberg, P. Emma, R. Rossmanith, "The North Arc of the SLC as a Spin Rotator", *Proc. of the 1993 Part. Acc. Conf*, Washington, DC (1993).

[Irwin 1993] J. Irwin, R. Helm, W.R. Nelson, D. Walz, "Conventional Collimation and Linac Protection", SLAC–PUB–6198 (May 1993).

[Brown 1977] K.L. Brown *et al.*, "TRANSPORT", SLAC–91 (May 1977).

[Carey 1982] D.C. Carey *et al.*, "Decay TURTLE", SLAC–246 (March 1982).

[Ziemann 1992] V. Ziemann, "Vacuum Tracking", SLAC–PUB–5962 (October 1992).

[Emma 1994] P. Emma, T. Limberg, R. Rossmanith, "Depolarization in the SLC Collider Arcs", *Proc. of the 1994 European Part. Accel. Conf.*, London, England (July 1994).

Contributors

- Paul Emma
- Dick Helm
- Tor Raubenheimer
- Mark Woodley